Progress In Electromagnetics Research C, Vol. 135, 95–106, 2023

Koch Snowflake Fractal Embedded Octagonal Patch Antenna with Hexagonal Split Ring for Ultra-Wide Band and 5G Applications

Aravindraj Ezhumalai[1, *], Nagarajan Ganesan[1], and Ramanathan Palaniappan[2]

Abstract—A Koch Snowflake fractal structure embedded octagonal patch antenna with a hexagonal split ring for Ultra-Wideband (UWB) and 5G applications is proposed. In this proposed design, Koch Snowflake pattern is chosen for embedding into the octagon-shaped patch antenna, which tentatively develops a miniaturized cross-sectional area in the radiator and introduces wide resonance with enhanced gain. The complete dimensions of the proposed model are $25 \times 30 \times 1.6\,\text{mm}^3$. The simulated design and fabricated prototype feature a Peak Gain of 6.3 dBi and 6.27 dB respectively; Fractional Bandwidth (FBW) of 168% (Frequency ranges from 2.6 GHz to 28.9 GHz) and 168% (Frequency ranges from 2.4 GHz to 28.5 GHz) respectively which are tested and measured using Microwave analyzer and anechoic chamber. Thus, the proposed antenna covers the resonance which includes S-band, C-band, X-band, Ku-band, and K-band. Also, it completely wraps the UWB spectrum range (3.1 GHz to 10.6 GHz), 5G (Sub-6 GHz band) Frequency Range 1 (FR 1) spectrum, and most deployed 5G mm-wave Frequency Range 2 (FR 2) spectrum (24.25 GHz to 29.5 GHz).

1. INTRODUCTION

The necessity of vamping vast microwave frequency sweep in antenna evolution has achieved a maximum extent in day-to-day existence. Instead of employing multiple radiating elements for various frequency ranges, usage of single component radiator that manages wider microwave frequencies may gratify the demand in radio communication advancements. The size and profile of the antenna should also be prominently considered in the case of mobile communication and other modern wireless environment. The conventional antennas may not effectively cover this eventuality. The diminished variant of the traditional antennas may not be efficacious to treat wide range of frequencies. Therefore, patch antennas are employed in certain situations where size miniaturization and dynamic utilization of wider frequencies are prerequisite. Generally, patch antennas are benevolent versions to function at low profile and capable to grip broader frequencies (Low to High) at less expense [1]. Although limitations like narrow bandwidth, impedance mismatch, and poor gain are quoted on conventional patch antennas, there are various advancements made on different sections of patch antennas to overcome their constraints. The implementation of fractal structures in the conventional patch antennas will miniaturize the size of the antenna and allow the antenna to operate from lower to higher frequency [2–4]; employing Flame Retardant 4 (FR4) as its dielectric medium for better reliability and mechanical strength [5]; implementation of Split ring resonators to the antenna design will engage LC tuning circuit which enhance the radiation effects of the antenna [6]; incorporating CPW feed and ground may enhance the bandwidth ratio and impedance bandwidth of the antenna [7].

In general, fractal structures are aroused from the codes of nature which recites at distinct scales. Fractal constructions are effectual patterns which can be appraised mathematically and physically from

Received 7 May 2023, Accepted 10 July 2023, Scheduled 27 July 2023
* Corresponding author: Aravindraj Ezhumalai (aravindraj1794@gmail.com).
[1] Department of Electronics and Communication Engineering, Pondicherry Engineering College, Puducherry, India. [2] Department of Electronics & Communication Engineering, Madanapalle Institute of Technology & Science, Andhra Pradesh, India.

various recursive self-similar structures. Based on their similarity pattern, fractal can be classified into Exact, Quasi, and Statistical self-similarity. Among the conventional fractal generating techniques, Iterated Function System (IFS) is employed for conceiving exactly self-similar structures in definite vertices. The self-similar dimensions can be obtained through Hausdroff dimension which are practiced in exact self-similar objects in metric space. These hyper-efficient fractal constructions with genetic algorithms are widely exerted in recent advancements in antenna engineering. Fractal patterns are embedded in patch antennas to significantly cut down the area of the antenna, magnify the effective length of the dielectric medium, and enhance the electromagnetic radiations around the entire surface volume [8]. The fractal editions deployed using IFS are: Koch Snowflake, Cantor set, Sierpinski Gasket, Sierpinski Carpet, Tree, Minkowski Island, Gosper Island, and some space filling curves [9, 10]. The resonance of the antenna is adopted and modified by selecting the suitable fractal design. The complex arrangements of self-inductance and capacitance cause current distribution slick around the radiating element. Due to reactive loading, the effective length may get higher, but the dimensions of the antenna remain same [11, 12].

An octagonal design is used as a patch will well the criteria suit, since shape of the patch will effectively dominate the current distribution on the radiating patch. Koch Snowflake fractal structure is opted in particular to miniaturize the dimension of the antenna within a triangle because in this fractal design the supplementary triangles created in next level iteration will fall within the same larger triangle [13]. An octagonal patch incorporated with a Koch Snowflake fractal structure will offer fine fringing fields and current distribution. The fringing fields are the proposals for the emission of electromagnetic waves from each nook of the radiating element. Among several feeding techniques, microstrip feed which probably allows decent impedance matching is utilized to carry radiating power from port to the patch of the antenna [14]. Co-planar waveguide (CPW) is implemented to enhance the fractional bandwidth (FBW) of the antenna. This CPW is also applied to attain circular polarization and control higher order harmonics. The dielectric medium or substrate is used for designing the Flame Retardant 4 (FR-4) which will provide physical stability and also produce displacement current [15]. The Proposed antenna is designed, simulated, and analyzed using High Frequency Structure Simulator (HFSS) tool [16].

The article is structured in such a way: Antenna Design Methodologies are characterized in Section 2 which contains Antenna Formulation, Koch snowflake configuration and Design Systematization. Section 3 presents the simulation outputs of the antenna and the experimental results of the fabricated prototype. Based on the comparison between the existing works and the proposed work, Section 4 provides the prime conclusion.

2. ANTENNA DESIGN METHODOLOGIES

The proposed antenna consists of an octagonal patch affixed on an FR4 substrate which is fed using a CPW cross section and a 3rd iteration level Koch fractal pattern engraved in the center of an octagonal patch, and a hexagonal spilt ring resonator is also inserted at the center of the patch which acts as an LC circuit. The design methodology incorporates antenna configuration of the octagonal patch antenna with Koch fractal implementation in octagonal patch and operating principle of generic antenna layout.

2.1. Antenna Formulation

The design methodology of the proposed layout stems from the generalized computations like determination of length and width of radiating element, dielectric medium, and ground. The values required for the calculations are operating frequency ($fr = 5.2\,\text{GHz}$), solidity of the substrate ($t = 1.6\,\text{mm}$), relative permittivity of the substrate (FR4) ($\varepsilon_r = 4.4$), and velocity of light ($C = 3 \times 10^8\,\text{m/s}$). The patch length and width are significant elements for designing a conventional patch radiator which initiates the dimensions of respective ground and substrate areas [17]. The primary expressions that denote the length and width of the patch are represented as W & L.

$$W = \frac{c}{2f_r\sqrt{\dfrac{(\varepsilon_r + 1)}{2}}} \tag{1}$$

$$L = \left[\frac{C}{2f_r\sqrt{\varepsilon_{eff}}}\right] - 2\left[\frac{0.412h\left(\varepsilon_{eff}+0.3\right)\left(\dfrac{W}{h}+0.264\right)}{\left(\varepsilon_{eff}-0.258\right)\left(\dfrac{W}{h}+0.8\right)}\right] \tag{2}$$

where the effective dielectric constant ε_{reff} is denoted as

$$\varepsilon_{eff} = \frac{\varepsilon_r+1}{2} + \frac{\varepsilon_r-1}{2}\left[1+12\frac{h}{W}\right]^{-1/2} \tag{3}$$

In the above equations, ε_{eff} is the effective dielectric constant which reports the effective length of the antenna.

Table 1 shows specifications and dimensions of the octagonal patch antenna, which has been created using High HFSS tool as shown in Figure 1. The octagonal patch antenna occupies the area of $25 \times 30 \times 1.6\,\text{mm}^3$ where the antenna is excited using a lumped port and bounded with an open region radiation boundary.

Table 1. Specifications and dimensions of octagonal patch antenna.

Antenna Section	Specification	Dimensions (mm)
Dielectric	Width (W_d)	25 mm
	Length (L_d)	30 mm
	Thickness (t)	1.6 mm
Patch	Side (a)	7.003 mm
	Circum Radius (R_c)	9.15 mm
CPW	Width (W_g)	11.1 mm
	Length (L_g)	7.8 mm
Slots (s1 & S2)	Width (W_s)	3.5 mm
	Length (L_s)	2.3 mm
Feed	Width (W_f)	1.8 mm
	Length (L_f)	8.72 mm

2.2. Implementation of Koch Snowflake Fractal

The Koch Snowflake fractals are exact self-similar structure which are developed using IFS technique with a generic algorithm. In this technique, the fractal patterns are mapped in a finite set of complete metric space using an affine transformation matrix which can be expressed as $V(x, y)$ [18].

$$V\begin{pmatrix} x \\ y \end{pmatrix} = \begin{pmatrix} a\cos\theta & c\sin\theta \\ b\sin\theta & d\cos\theta \end{pmatrix}\begin{pmatrix} x \\ y \end{pmatrix} + \begin{pmatrix} x_0 \\ y_0 \end{pmatrix} \tag{4}$$

With considering the increasing level contraction factor n, the geometry of the structure is framed using a set of complex linear matrix which is portrayed as Hutchinson operator (V), and it regulates the vertices of the respective iteration levels [19].

$$V[A] = \bigcup_{n=1}^{3} V_n(A) \tag{5}$$

A generic Hausdroff-Besicovitch formula is used to define the position of fractal pattern in the Euclidean dimension (D) which declines its narrow scale by reversing the scaling factor (S) and balance the number

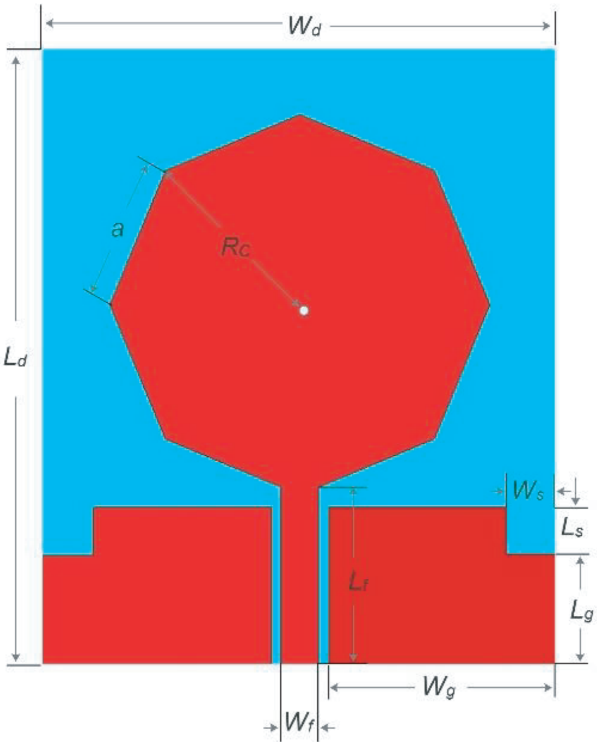

Figure 1. Specifications of octagonal patch antenna.

of increasing self-identical branch count (N) [20]. Thus, the Hausdroff-Besicovitch can be expressed as

$$N = S^D \tag{6}$$

$$\log_{10}\varepsilon(N) = D\log_{10}(S) \tag{7}$$

By simplifying the Hausdroff-Besicovitch equation towards Euclidean dimension (D), the expression for generating Koch Snowflake pattern can be represented with the scaling factor of 3 and number of self-identical counts of 4 which in-turn offers the Hausdroff-Besicovitch measure for Koch fractal structure.

$$D = \frac{\log_{10}(N)}{\log_{10}(S)} \tag{8}$$

$$D = \frac{\log_{10}(N)}{\log_{10}(S)} = \frac{\log_{10}(4)}{\log_{10}(3)} = 1.261 \tag{9}$$

The geometry of Koch Snowflake template begins with an equilateral triangle. For iteration level 1, the initial triangle has been segmented into one-third in each side, and the corresponding lengths are arranged in such a way to form another equilateral triangle as its branch [21].

The proportionate values for the first iteration of Koch fractal are plotted in the affine transformation matrices to achieve the finite points and positions of the structure in the vertices [22]. Figure 2 shows a three-level increasing order iterations of Koch Snowflake fractal pattern.

2.3. Operating Principle

The eventual design consists of an octagonal patch with an ingrained Koch fractal design and hexagonal split ring where the foresaid framework is fed using a CPW feeding technique. As represented in Section 2.2, the Koch Snowflake pattern with third order iterative level which is constructed using IFS technique is implemented in the octagonal patch to support size miniaturization and foster the radiation of the antenna. The entire dimension of the antenna is $25 \times 30 \times 1.6\,\mathrm{mm}^3$. Figures 3(a) and 3(b) show the simulated and fabricated octagonal Koch Snowflake fractal antennas, respectively.

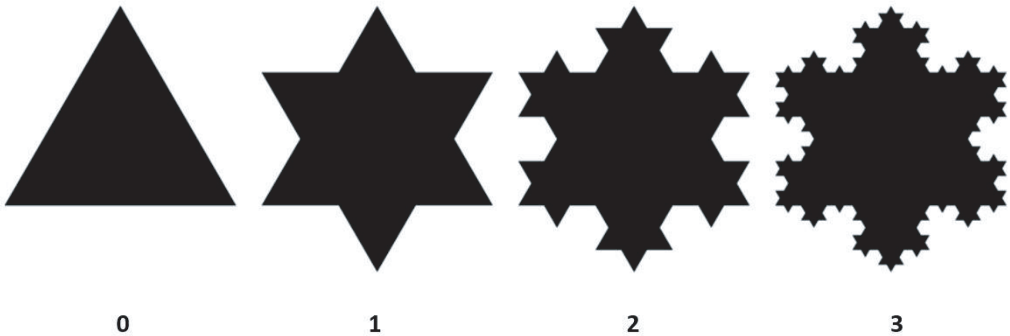

Figure 2. Increasing levels of Koch Snowflake Fractal pattern.

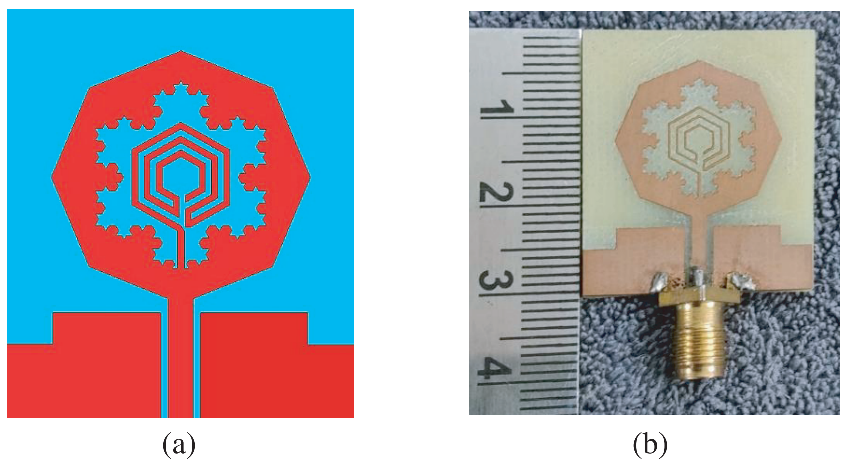

Figure 3. Simulated and fabricated octagonal Koch Snowflake Fractal antenna.

3. RESULTS AND DISCUSSIONS

3.1. Return Loss and Bandwidth

Observing the S_{11} parameter of simulated and experimented antennas, it is inferred that both the antennas deliver a wide bandwidth and offer a legitimate agreement with each other. The suspended fractal structure embedded in the octagonal design and edge slits S_1 and S_2 in the CPW were used to increase bandwidth in the proposed design. Cutting truncation and cut edge employed in the octagonal patch embedded Koch fractal will prompt more discontinuity in the directed radiation, and progressive reflections will eventually result in better bandwidth. In this proposed antenna design, the edge truncation in the patch provides efficient reflection and current distribution at the boundary of patch. Here, -10 dB is the reference range for an antenna to produce operable frequencies. From S_{11} plot shown in Figure 4, it is recognized that the simulated antenna operates at the resonance bandwidth of 2.5 GHz to 28.9 GHz, and the fabricated prototype functions at 2.4 GHz to 28.5 GHz.

3.2. Voltage Standing Wave Ratio (VSWR)

Voltage Standing Wave Ratio (VSWR) is a significant measure to indicate the radio power mismatch from the transmission line to the radiating element. The same as reflection coefficient, VSWR also has a reference point (i.e., VSWR = 2), and the rate should not fall below 1. From the plot shown in Figure 5, it is noticed that the simulated and fabricated prototypes operate at the resonance of 2.5 GHz to 28.9 GHz and 2.4 GHz to 28.5 GHz, respectively.

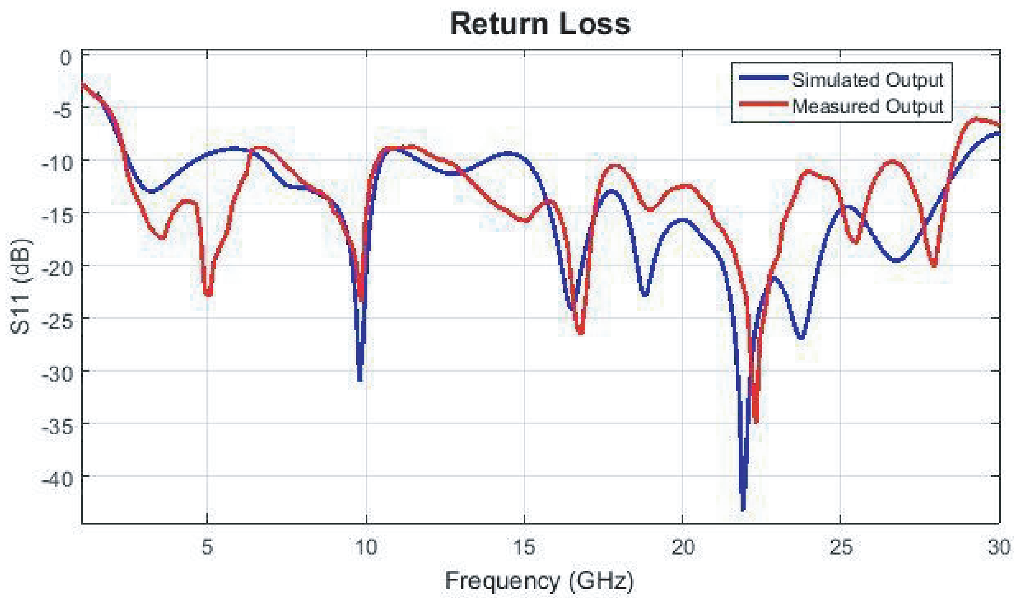

Figure 4. Simulated and measured return loss.

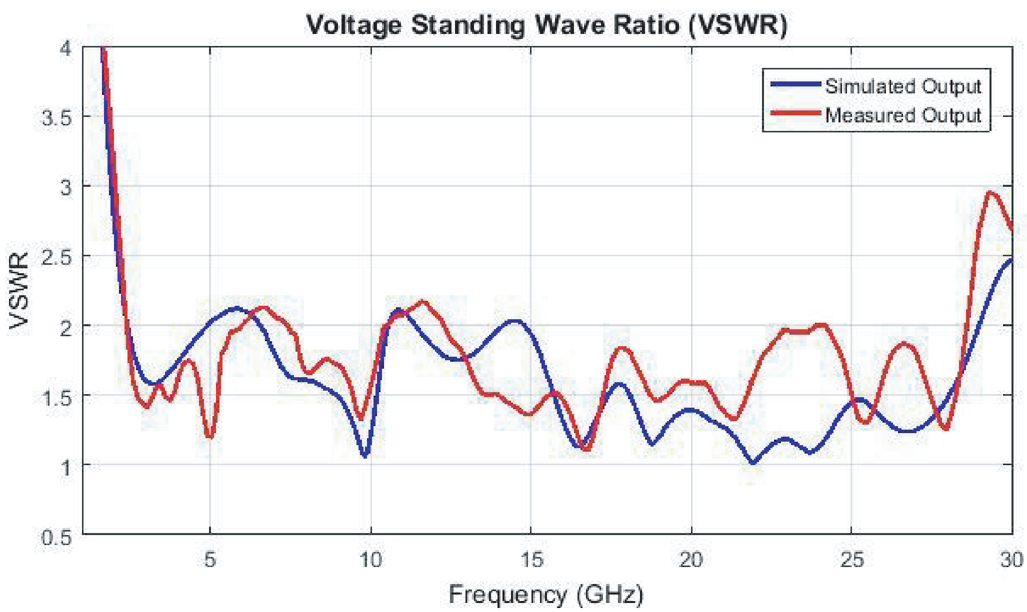

Figure 5. Simulated and measured VSWR.

3.3. Gain

The gain of the simulated antenna is represented in Figure 6. From the 3D-pattern of the gain, it is known that the radiation of the antenna has achieved an omnidirectional pattern, where the antenna is capable of radiating in all 360 degrees at 18 GHz. The simulated antenna offered a peak gain value of 6.3 dBi at 18 GHz.

The peak gain observed from the proposed octagonal Koch fractal antenna over the end-to-end frequency range (2.5 GHz to 28.9 GHz) is shown in Figure 7. By observing the gain chart, it is noted that the simulated Koch fractal antenna achieved a peak gain of 6.29 dBi at 18 GHz.

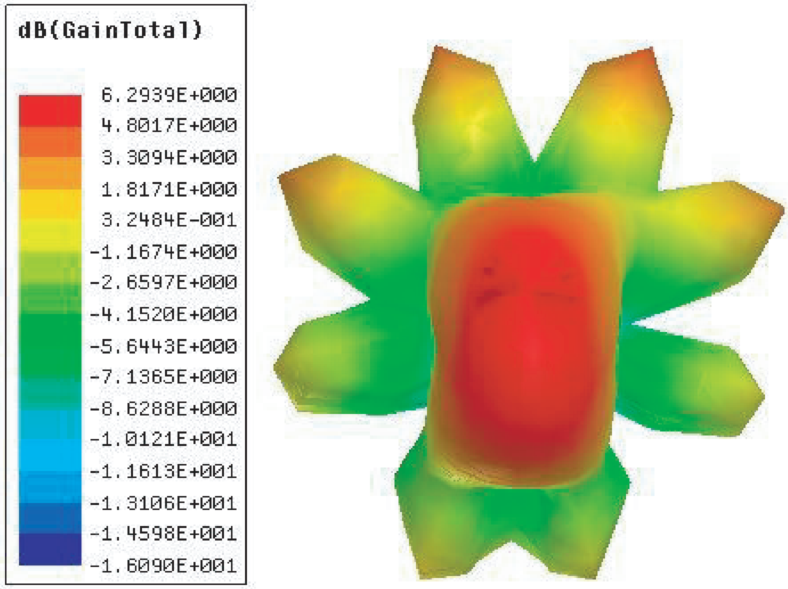

Figure 6. Simulated gain.

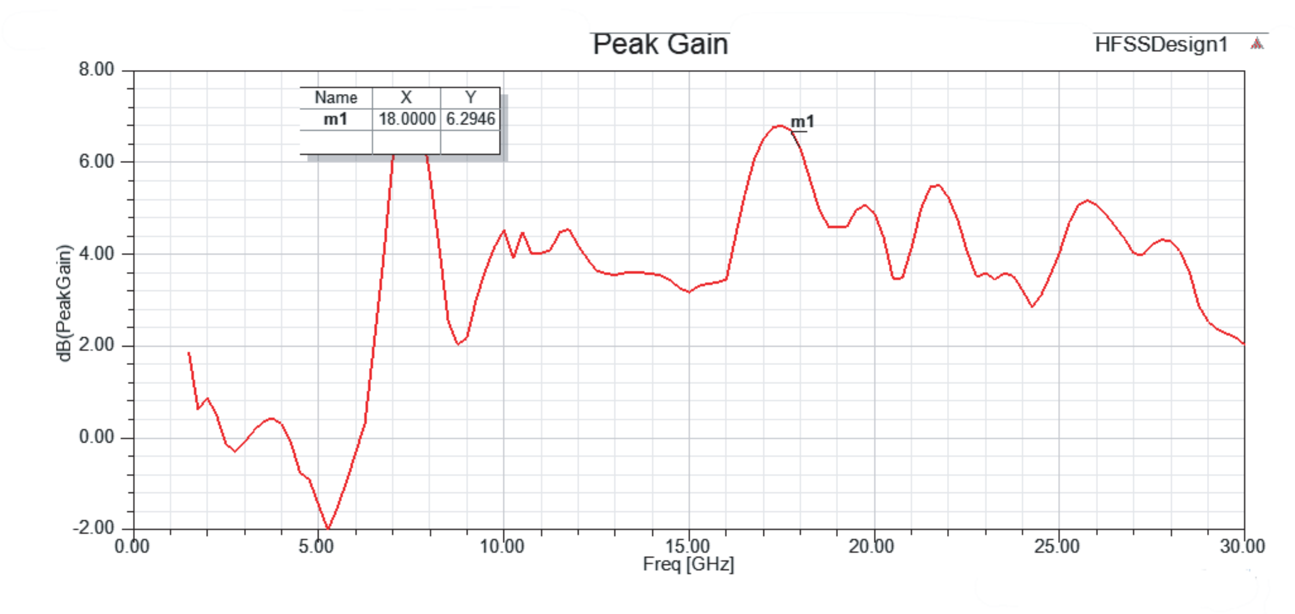

Figure 7. Peak gain observed from the Koch fractal antenna.

3.4. Radiation Pattern

The 2-D radiation patterns at elevation and azimuth angles are denoted in Figure 7 and Figure 8 respectively. At elevation angle, the radiation pattern when θ varies from 0° to 360° and φ is fixed at 0° and 90° is shown in Figure 8(a), and the radiation pattern when θ varies from 0° to 360° and φ is fixed at 90° and 180° is shown in Figure 8(b). At azimuth angle, the radiation pattern when φ varies from 0° to 360° and θ is fixed at 0° and 90° is shown in Figure 9(a), and the radiation pattern when φ varies from 0° to 360° and θ is fixed at 90° and 180° is shown in Figure 9(b).

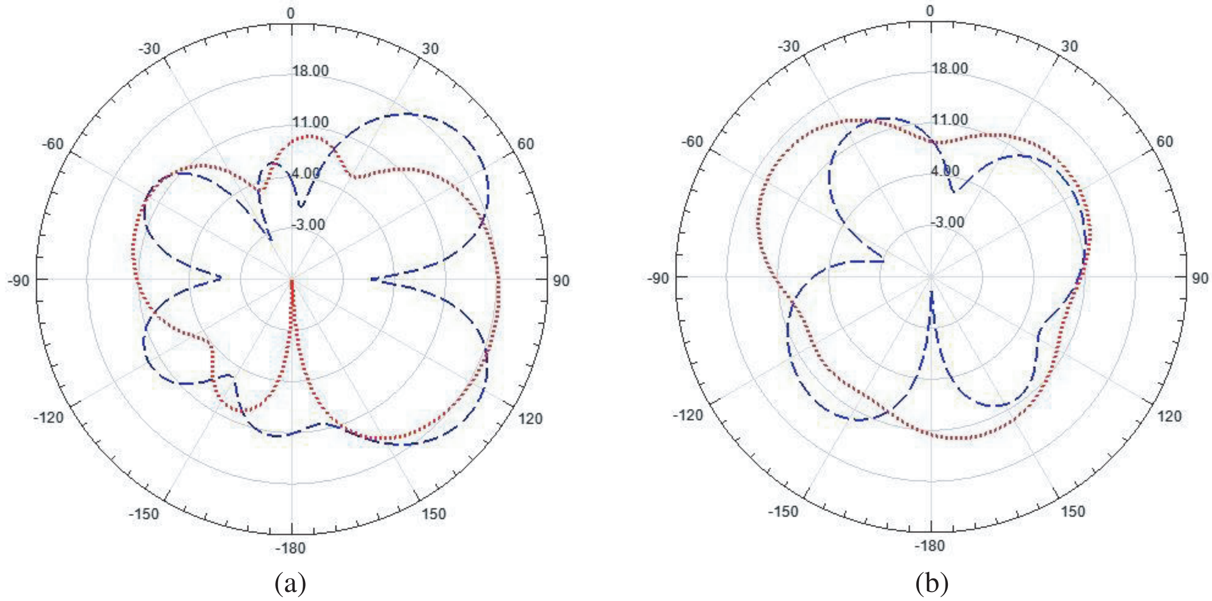

Figure 8. 2-D radiation pattern at elevation angle. (a) $\varphi = 0°$ to $360°$; $\theta = 0°$ and $90°$. (b) $\varphi = 0°$ to $360°$; $\theta = 90°$ and $180°$.

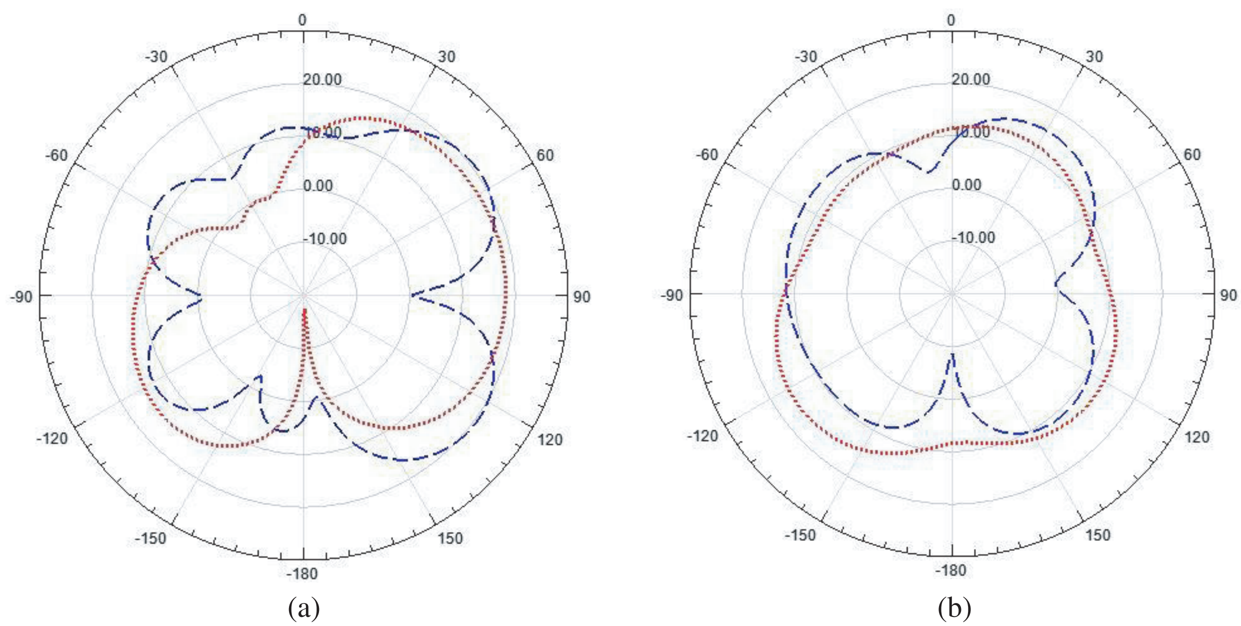

Figure 9. 2-D radiation pattern at azimuth angle. (a) $\theta = 0°$ to $360°$; $\varphi = 0°$ and $90°$. (b) $\theta = 0°$ to $360°$; $\varphi = 90°$ and $180°$.

3.5. Anechoic Chamber Measurement

On experimenting the antenna prototype, the fabricated antenna will be placed at the receiver end which is 2-meters away from the transmitting antenna in E-plane as shown in the Figures 10(a) and 10(b), and H-plane is shown in Figures 10(c) and 10(d). The gain is measured in terms of power (dB) in an anechoic chamber where the fabricated antenna prototype is placed in the receiver station, and the received power is measured at both E and H planes as shown in Figures 10(a), (b) and Figures 10(c), (d), respectively.

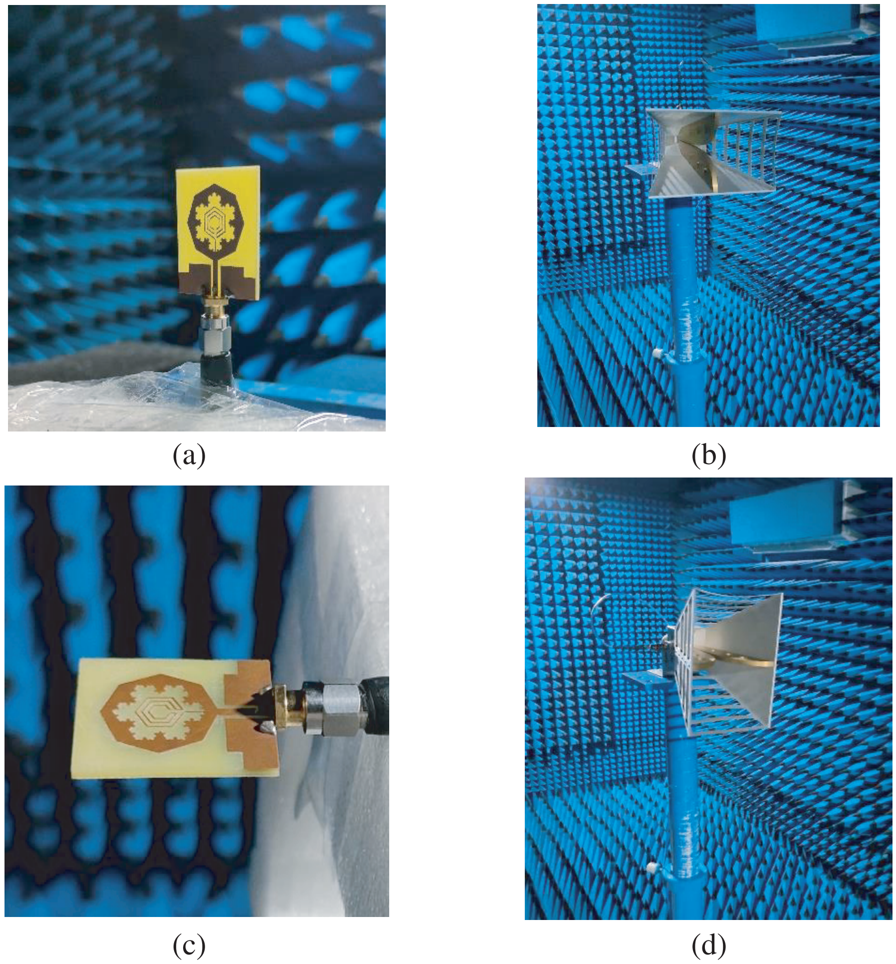

Figure 10. *E*-Plane and *H*-Plane arrangement of experimented antenna in an-echoic chamber.

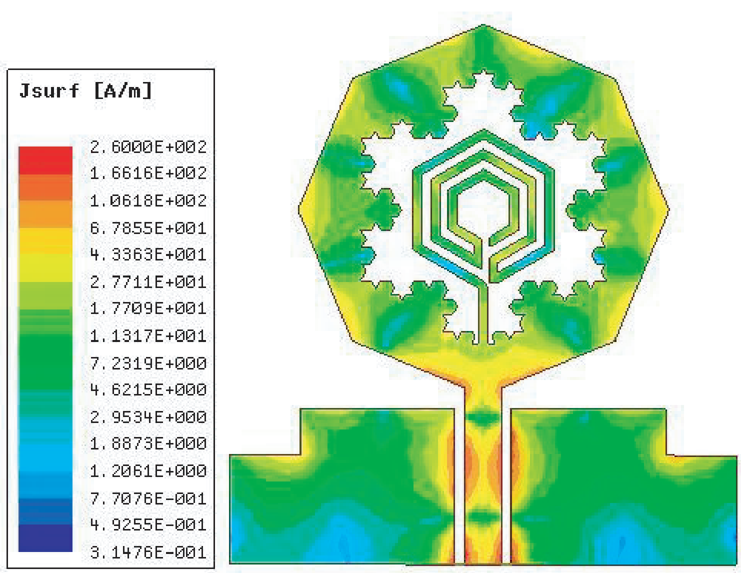

Figure 11. Simulated current distribution.

3.6. Current Distribution and Impedance Matching

The current dispensation of the simulated antenna is shown in Figure 11 emphasizes the electric field distribution in the surface of the octagonal patch and CPW ground. The current distribution is measured at the resonance of 18 GHz. This parameter depicts the power levels at the corners and edges of the antenna. The impedance of the simulated antenna is practically obtained and shown in Figure 12.

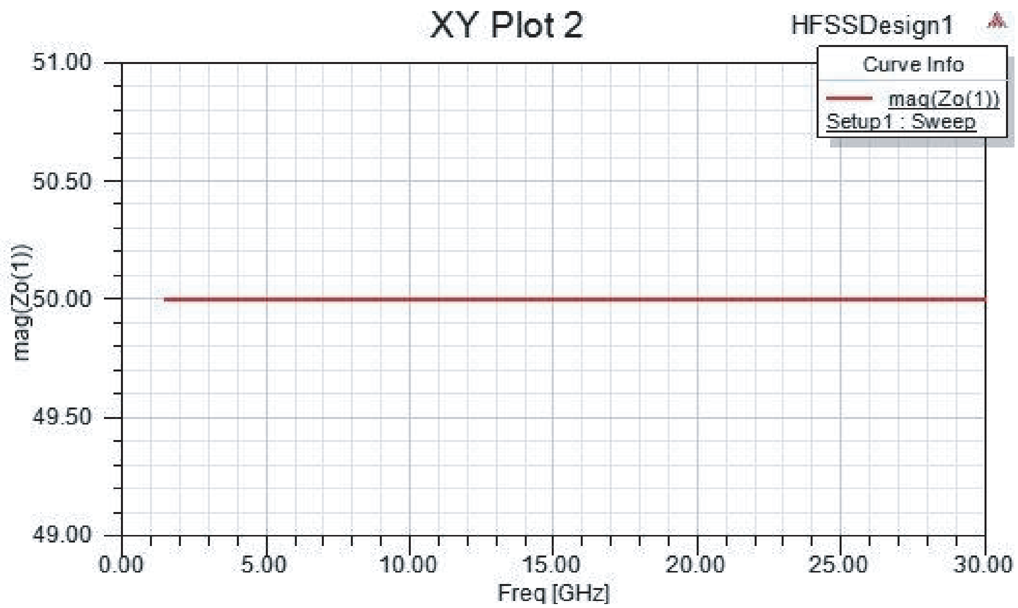

Figure 12. Simulated input impedance.

In Table 2, the proposed work is compared with some recent existing works. Here, the parameters like dimension of the antenna, frequencies radiated by the antenna, and fractional bandwidth and gain of the antenna are considered for comparison. The table clearly illustrates that the proposed antenna offers enhanced output parameters.

Table 2. Comparison of proposed work with some recent existing works.

Ext./Prop. Work	Dimensions (mm^3)	Frequency Range (GHz)	FBW (%)	Gain (dB)	BW ratio
[23]	$38 \times 36 \times 1.4$	3–21.5	151	5	7.16 : 1
[24]	$34 \times 34 \times 1.6$	2.4, 3.1, 4.8 & 5.6	35	4.02	2.1 : 1
[25]	$30 \times 30 \times 1.6$	5.8–7.47	45.6	3.79	1.28
[26]	$52 \times 46 \times 1.6$	2.2–8.4	116.9	4.4	3.81 : 1
[27]	$30 \times 30 \times 1.6$	2.8–5.6	66.6	5.09	2 : 1
[28]	$120 \times 120 \times 1.6$	1.45–4.86	108	5.8	3.35 : 1
[29]	$32 \times 36 \times 1.6$ mm	2.23–17.29	154	3.23	4.21 : 1
[30]	$24 \times 30 \times 1.6$ mm	2.19–11.32	149	4.19	5.62 : 1
[31]	$30 \times 30 \times 1.6$	4.1–19.8	131	6.1	4.8 : 1
Sim. results	$\mathbf{25 \times 30 \times 1.6}$	**2.5–28.9**	**168**	**6.3**	**11.5 : 1**
Expt. results	$\mathbf{25 \times 30 \times 1.6}$	**2.4–28.5**	**168**	**6.27**	**11.8 : 1**

4. CONCLUSION

In this proposed work, a nature inspired Koch Snowflake pattern is embedded into an octagon-shaped patch antenna with a hexagonal split ring and co-planar waveguide (CPW). The simulated design features a peak gain of 6.3 dBi and fractional bandwidth (FBW) of 168% (Frequency ranges from 2.6 GHz to 28.9 GHz) with bandwidth ratio of 11.1 : 1. Also, the fabricated prototype offers FBW of 168% (2.4 GHz to 28.5 GHz) and gain of 6.27 dB which are tested and measured using Microwave Analyser and anechoic chamber, respectively. Thus, the operating frequencies of the proposed antenna cover S-band, C-band, X-band, Ku-band, and K-band. Also, it completely covers the ultra-wideband (UWB) spectrum range (3.1 GHz to 10.6 GHz), 5G (Sub-6 GHz band) Frequency Range 1 (FR 1) spectrum, and most deployed 5G mm-wave Frequency Range 2 (FR 2) spectrum (24.25 GHz to 29.5 GHz).

REFERENCES

1. Balanis, C. A., *Antenna Theory: Analysis and Design*, John Wiley & Sons, 2015.
2. Barnsley, M. F., *Fractals Everywhere*, Academic Press, 2014.
3. Iqbal, A., A. Smida, N. K. Mallat, M. T. Islam, and S. Kim, "A compact UWB antenna with independently controllable notch bands," *Sensors*, Vol. 19, No. 6, 1–12, 2019.
4. Ahmad Jan, N., S. Hassan Kiani, D. Ali Sehrai, M. Rizwan Anjum, and A. Iqbal, "Design of a compact monopole antenna for UWB applications," *Computers, Materials* & *Continua*, Vol. 66, No. 1, 35–44, 2021.
5. Aravindraj, E., K. Ayyappan, and R. Kumar, "Performance analysis of rectangular MPA using different substrate materials for WLAN application," *ICTACT Journal on Communication Technology*, Vol. 8, No. 1, 1447–1452, 2017.
6. Rajalakshmi, P. and N. Gunavathi, "Hexagonal split ring resonator enclosed circular split ring resonator inspired dual-band antenna for sub-6 GHz 5G NR and IEEE 802.11ba/Be applications," *Progress In Electromagnetics Research C*, Vol. 115, 1–15, 2021,
7. Abbaoui, H., A. Ghammaz, H. Belahrach and R.-J. El Bakouchi, "Design and simulation of a low return loss UWB CPW-fed patch antenna for mobile wireless communications," *International Conference on Connected Object and Artificial Intelligence*, Vol. 52, 1–11, 2023.
8. Aravindraj, E., G. Nagarajan, and B. Sathishkumar, "An extensive survey on fractal structures using iterated function system in patch antennas," *International Journal of Communication Systems* Vol. 34, No. 15, 1–38, 2021.
9. Mandelbrot, B. B., *The Fractal Geometry of Nature*, WH Freeman New York, 1982.
10. Falconer, K. J., *Techniques in Fractal Geometry*, Wiley Chichester, 1997.
11. Awan, W. A., A. Zaidi, N. Hussain, A. Iqbal, and A. Baghdad, "Stub loaded, low profile UWB antenna with independently controllable notch-bands," *Microwave and Optical Technology Letters*, Vol. 61, No. 11, 2447–2454, 2019.
12. Kundu, S., A. Chatterjee, and A. Iqbal, "Printed circular ultra-wideband antenna with triple sharp frequency notches for surface penetrating radar application," *Sādhanā*, Vol. 45, No. 4, 1–7, 2020.
13. Elavarasi, C. and T. Shanmuganantham, "Multiband SRR loaded koch star fractal antenna," *Alexandria Engineering Journal*, Vol. 57, No. 3, 1549–1555, 2018.
14. Selas, W. S. and K. Ayyappan, "Design of rectangular MPA with and without split ring resonators for WLAN application," *2020 International Conference on Computer Communication and Informatics (ICCCI)*, 1–5, IEEE, 2020.
15. Aravindraj, E. and K. Ayyappan, "Design of slotted H-shaped patch antenna for 2.4 GHz WLAN applications," *2017 International Conference on Computer Communication and Informatics (ICCCI)*, 1–5, IEEE, 2017.
16. Aravindraj, E., A. Kannan, and K. Ayyappan, "Performance of rectangular microstrip patch antenna in two different design tools-a comparative study," *International Journal of Scientific Research in Science, Engineering and Technology*, Vol. 5, No. 3, 2018.

17. Aravindraj, E., G. Nagarajan, and R. Senthil Kumaran, "Design and analysis of recursive square fractal antenna for WLAN applications," *2020 International Conference on Emerging Trends in Information Technology and Engineering (IC-ETITE)*, 1–5, IEEE, 2020.
18. Paun, M.-A., M.-V. Nichita, V.-A. Paun, and V.-P. Paun, "Fifth-generation fractal antenna design based on the Koch Snowflake geometry," *A Fractal Theory Application*, Early issue, e13242, 2023.
19. Yadav, K., A. Jain, N. M. O. S. Ahmed, S. A. S. Hamad, G. Dhiman, and S. D. Alotaibi, "Internet of thing based Koch Fractal curve fractal antennas for wireless applications," *IETE Journal of Research*, Vol. 22, No. 4, 1–10, 2022.
20. Choukiker, Y. K. and S. K. Behera, "Wideband frequency reconfigurable Koch snowake fractal antenna," *IET Microwaves, Antennas & Propagation*, Vol. 11, No. 4, 203–208, 2017.
21. Gobinath, A., N. Sureshkumar, K. K. Hema, T. Sureka, and B. Pavithra, "Design of Koch Fractal antenna for wireless applications," *International Journal of Engineering Research & Technology*, Vol. 5, No. 9, 1–3, 2023.
22. Kumar, A. P. and G. Kiran Kumar, "Modified Koch curve with beeline fractal antenna for 5G communication system," *2022 IEEE 19th India Council International Conference (INDICON)*, 1–4, Kochi, India, 2022.
23. Dastranj, A., F. Ranjbar, and M. Bornapour, "A new compact circular shapefractal antenna for broadband wireless communication applications," *Progress In Electromagnetics Research C*, Vol. 93, 19–28, 2019.
24. Bhilegaonkar, P. and S. Bansod, "A compact hybrid fractal antenna using Koch and Minkowski curves for wireless applications," *International Journal of Engineering Research Technology*, Vol. 10, No. 6, 185–188, 2021.
25. Mythili, S., K. Akshaya, B. Charanya, and K. Ayyappan, "Design and analysis of Koch fractal antenna for WLAN applications," *ICTACT Journal on Microelectronics*, Vol. 6, No. 2, 923–927, 2020.
26. Orugu, R. and N. Moses, "Triangular fractal loaded reconfigurable antennawith notch band characteristics," *International Journal of Numerical Modelling: Electronic Networks, Devices and Fields*, Vol. 34, No. 1, 1–11, 2021.
27. Annou, A., S. Berhab, and F. Chebbara, "Metamaterial-fractal-defected ground structure concepts combining for highly miniaturized triple-band antenna design," *Journal of Microwaves, Optoelectronics and Electromagnetic Applications*, Vol. 19, 522–541, 2020.
28. Liu, G., J. Gu, Z. Gao, and M. Xu, "Wideband printed slot antenna usingkoch fractal metasurface structure," *International Journal of RF and Microwave Computer-Aided Engineering*, Vol. 30, No. 3, 1–6, 2020.
29. Bharti, G. and J. S. Sivia, "a design of multiband nested square shaped ring fractal antenna with circular ring elements for wireless applications," *Progress In Electromagnetics Research C*, Vol. 108, No. 12, 115–125, 2021.
30. Benkhadda, O., M. Saih, S. Ahmad, A. J. A.Al-Gbur, Z. Zakaria, K. Chaji, and A. Reha, "A miniaturized tri-wideband Sierpinski hexagonal-shaped fractal antenna for wireless communication applications," *Fractal and Fractionals*, Vol. 7, No. 2, 1–18, 2023.
31. Aravindraj, E., G. Nagarajan, and R. S. Kumaran, "A monopole octagonal Sierpinski carpet antenna with defective ground structure for SWB applications," *Machine Learning, Deep Learning and Computational Intelligence for Wireless Communication*, Vol. 749, 267–280, Springer, 2021.